Rapid Communications

Generic features of the neutron-proton interaction

Y. H. Kim,* M. Rejmund, P. Van Isacker, and A. Lemasson
GANIL, CEA/DRF-CNRS/IN2P3, Bd Henri Becquerel, BP 55027, F-14076 Caen Cedex 5, France

(Received 7 September 2017; revised manuscript received 21 December 2017; published 4 April 2018)

We show that fully aligned neutron-proton pairs play a crucial role in the low-energy spectroscopy of nuclei with valence nucleons in a high-j orbital. Their dominance is valid in nuclei with valence neutrons and protons in different high-j orbitals as well as in $N = Z$ nuclei, where all nucleons occupy the same orbital. We demonstrate analytically this generic feature of the neutron-proton interaction for a variety of systems with four valence nucleons interacting through realistic, effective forces. The dominance of fully aligned neutron-proton pairs results from the combined effect of (i) angular momentum coupling and (ii) basic properties of the neutron-proton interaction.

DOI: 10.1103/PhysRevC.97.041302

Insight into the properties of correlated quantum many-body systems often can be obtained by means of solvable models. In condensed-matter physics arguably the most important example is the Hubbard model, for which an exact solution is known in one dimension [1]; many other examples are reviewed in Ref. [2]. In nuclear physics, solvable models fall into two broad classes, depending on whether the nucleons interact through a pairing or a quadrupole force. The former case, first considered by Racah in the context of atomic physics [3], applies to "semimagic" nuclei with either neutrons or protons in the valence shell, and leads to a classification of states in terms of seniority or, equivalently, in terms of the number of unpaired nucleons. The quadrupole force, on the other hand, is appropriate for nuclei with several neutrons *and* protons in the valence shell, and gives rise to a rotational classification of states based on SU(3) symmetry [4]. While their solution may be exact, such models provide at best approximations to observed quantum many-body systems.

Some time ago Cederwall *et al.* [5] suggested that in self-conjugate nuclei (i.e., $N = Z$ nuclei with equal numbers of neutrons and protons) yet a different classification scheme may exist. Although not based on the property of solvability, their analysis claimed an analogy with pairing: While in traditional pairing models states are analyzed in terms of $J = 0$ pairs composed of either two neutrons ($\nu\nu$) or two protons ($\pi\pi$), the approach of Cederwall *et al.* centered on neutron-proton ($\nu\pi$) pairs that are fully aligned in angular momentum, which we refer to as fully aligned $\nu\pi$ pairs (FAPs). The claim for the existence of this novel coupling scheme was based on the measured spectrum of $^{92}_{46}\mathrm{Pd}_{46}$ and backed by a theoretical analysis in the framework of the nuclear shell model [6,7]. The idea of FAPs (which also relates to the stretch scheme proposed by Danos and Gillet [8]) provoked a flurry of studies based on boson mappings [9,10] or symmetry techniques [11,12], or with the use of schematic interactions [13–15] in a single-j approach. Simultaneously, also multi-j calculations with realistic interactions were carried out [16–20] to test the prevalence of FAPs in $N = Z$ nuclei. A review can be found in Ref. [21]. Despite occasional contradictions, a general consensus seems to have emerged that FAPs are dominant (with some caveats, see below) if neutrons and protons occupy a single-j orbital but that their dominance fades away quickly in a multi-j scenario. In addition, it has also become clear that the different proposed schemes are not mutually exclusive because of their nonorthogonality, and that, for example, nuclear ground states can be equally well described in terms of $J = 0$ and $J = 1$ pairs [19].

It should nevertheless be stressed that studies of the FAP conjecture so far have been limited to $N = Z$ nuclei. In this Rapid Communication we point out that FAP dominance is a widely occurring phenomenon, not confined to the restricted class of $N = Z$ nuclei, but present throughout the nuclear chart whenever valence neutrons and protons mainly occupy high-j orbitals. We show that the FAP dominance results from the combined effect of (i) angular momentum coupling and (ii) some basic properties of the $\nu\pi$ interaction.

We consider nuclei with neutrons and protons in valence orbitals j_ν and j_π, respectively, and concentrate on nuclei with two neutrons and two protons $(2 + 2)$, briefly exploring at the end the case $(4 + 4)$. The relevant $\nu\nu$, $\pi\pi$, and $\nu\pi$ two-body matrix elements (TBMEs) of the residual interaction are denoted by $V^{J_\nu}_{\nu\nu}$, $V^{J_\pi}_{\pi\pi}$, and $V^{J_{\nu\pi}}_{\nu\pi}$, respectively, where J_ν, J_π, and $J_{\nu\pi}$ are the coupled angular momenta of two nucleons. For a nucleus with two neutrons and two protons in the valence orbitals, the matrix element of the Hamiltonian in a $\nu\nu$-$\pi\pi$ basis with vectors $|J_\nu J_\pi; J\rangle$ can be expressed in terms of the TBMEs as follows:

$$\langle J_\nu J_\pi; J|\hat{H}|J'_\nu J'_\pi; J\rangle = \left(V^{J_\nu}_{\nu\nu} + V^{J_\pi}_{\pi\pi}\right)\delta_{J_\nu J'_\nu}\delta_{J_\pi J'_\pi} + \sum_{J_{\nu\pi}} C_{J_{\nu\pi}} V^{J_{\nu\pi}}_{\nu\pi}, \quad (1)$$

where $C_{J_{\nu\pi}} \equiv C_{J_{\nu\pi}}(j_\nu, j_\pi, J_\nu, J_\pi, J'_\nu, J'_\pi, J)$ is an angular-momentum coupling coefficient, whose explicit expression is given in the Supplemental Material [22]. Note that the $\nu\nu$

*yunghee.kim@ganil.fr

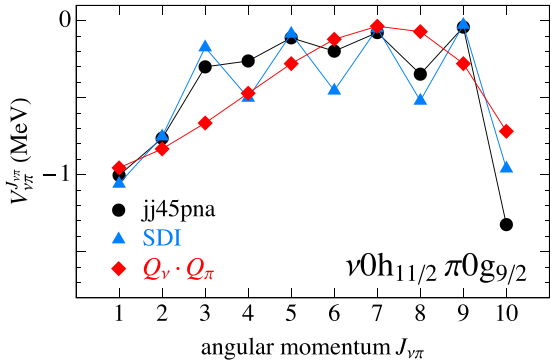

FIG. 1. TBMEs for three different $\nu 0h_{11/2}\pi 0g_{9/2}$ interactions: (i) realistic (jj45pna, black circles), (ii) surface delta (SDI, blue triangles), and (iii) quadrupole ($Q_\nu \cdot Q_\pi$, red squares).

and $\pi\pi$ interactions contribute only to Hamiltonian matrix elements that are diagonal, and that solely the $\nu\pi$ interaction is responsible for the mixing in the $\nu\nu$-$\pi\pi$ basis.

In the following we present a detailed discussion of ^{128}Cd, which has two proton and two neutron holes with respect to the closed-shell nucleus ^{132}Sn and we assume that the low-energy states are dominated by the high-j intruder orbitals $\nu 0h_{11/2}$ and $\pi 0g_{9/2}$. This assumption can be verified in a large-scale shell-model calculation with a realistic residual interaction and a valence space consisting of $\nu 1d_{3/2}$, $2s_{1/2}$, $0h_{11/2}$, and $\pi 1p_{1/2}$,$0g_{9/2}$ [23]. For the positive-parity yrast states with J^π from 0^+ to 18^+, the calculated occupation probabilities of $\nu 0h_{11/2}$ and $\pi 0g_{9/2}$ are $\gtrsim 10$ and $\gtrsim 8$, respectively, which strongly support our assumption. The $\nu\nu$ and $\pi\pi$ TBMEs are set so as to reproduce the experimental spectra of ^{130}Sn and ^{130}Cd, respectively. To test the robustness of our hypothesis concerning the FAP dominance, we use three different $\nu\pi$ TBMEs shown in Fig. 1: (i) the realistic interaction jj45pna [24], (ii) a surface delta interaction (SDI) with isoscalar and isovector strengths adjusted to jj45pna, and (iii) a quadrupole interaction $Q_\nu \cdot Q_\pi$ (plus a constant). The latter schematic interaction is included here to study its relation to the FAP scheme [25].

In Fig. 2 the coefficient $C_{J_{\nu\pi}}$ in Eq. (1) is shown as a function of $J_{\nu\pi}$ for $J = 0$ and $J = 2$. This coefficient strongly suppresses the contribution of low-$J_{\nu\pi}$ interactions and favors the interaction in the state with angular momentum $J_{\nu\pi}^{\rm FAP} \equiv j_\nu + j_\pi$. This is so in particular for $J = J_\nu = J_\pi = J'_\nu = J'_\pi = 0$, in which case $C_{J_{\nu\pi}}$ is proportional to $2J_{\nu\pi} + 1$. The contribution of the FAP is strongest also for the off-diagonal matrix elements and therefore dominates the mixing in the $\nu\nu$-$\pi\pi$ basis. This is further illustrated in Fig. 2 by showing the energy contribution in the $\nu\nu$-$\pi\pi$ basis due to the jj45pna TBMEs as a function of $J_{\nu\pi}$ for $J = 0$ and $J = 2$. The only significant contribution is observed for the FAP while the low-$J_{\nu\pi}$ interactions represent a nearly constant, small contribution.

In Fig. 3 are shown the yrast levels resulting from the diagonalization of the Hamiltonian matrix (1) with the full $\nu\nu$ and $\pi\pi$ interactions but with only a single nonzero component $J_{\nu\pi}$ ($V_{\nu\pi}^{J\neq J_{\nu\pi}} = 0$) of the above-mentioned $\nu\pi$ interactions. The levels are shown as a function of $J_{\nu\pi}$ and compared to those obtained with the full Hamiltonian as well as to

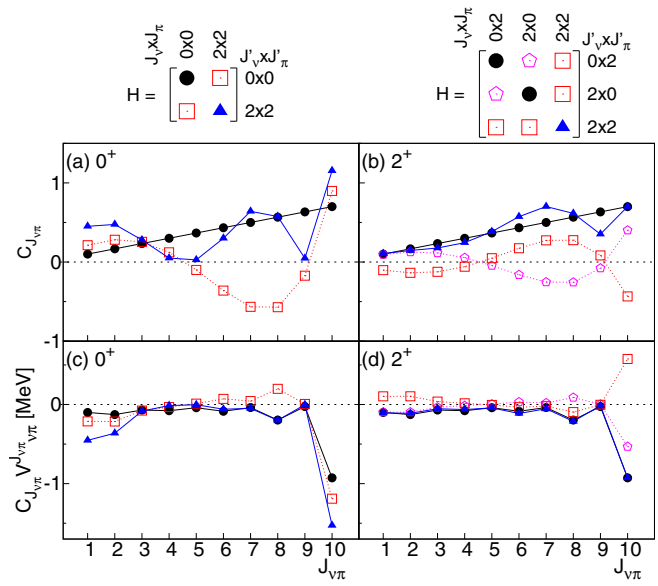

FIG. 2. Panels (a) and (b): The coefficient $C_{J_{\nu\pi}}$ in Eq. (1) for $j_\nu = 11/2$ and $j_\pi = 9/2$ as a function of $J_{\nu\pi}$ for $J = 0$ and $J = 2$. Panels (c) and (d): The energy contribution in the $\nu\nu$-$\pi\pi$ basis due to the individual TBMEs of the jj45pna interaction as a function of $J_{\nu\pi}$ for $J = 0$ and $J = 2$. Different symbols correspond to various couplings $(J_\nu, J_\pi, J'_\nu, J'_\pi)$ as indicated. Full (open) symbols indicate diagonal (off-diagonal) matrix elements in the $\nu\nu$-$\pi\pi$ basis.

the experimental results. Clearly, the interaction in the FAP state has the crucial impact on the level energies, and this is so for the three interactions. The close agreement between observed level energies and those calculated with the jj45pna interaction further justifies the assumption that the structure of the low-energy states is dominated by the high-j intruder orbitals $\nu 0h_{11/2}$ and $\pi 0g_{9/2}$. The correspondence between the spectra calculated with a single non-zero component $J_{\nu\pi} = 10$

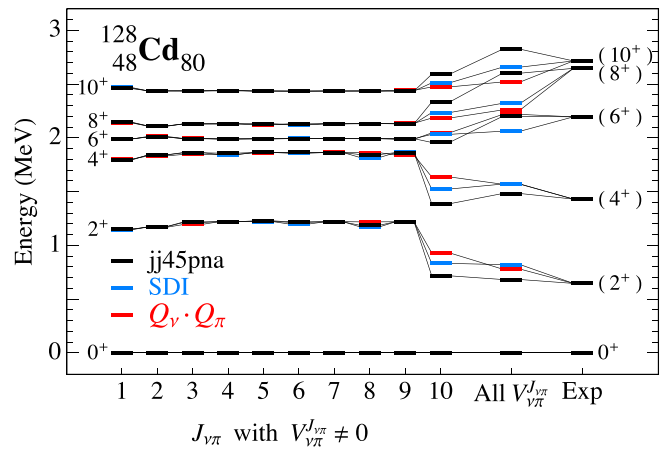

FIG. 3. Energies of the yrast eigenstates of the Hamiltonian (1) for two neutrons and two protons (^{128}Cd) as a function of $J_{\nu\pi}$, the angular momentum of the only nonzero component in the $\nu\pi$ interaction ($V_{\nu\pi}^{J_{\nu\pi}} \neq 0$). The results are for three different $\nu\pi$ interactions: (i) realistic (jj45pna, black), (ii) surface delta (SDI, blue), and (iii) quadrupole ($Q_\nu \cdot Q_\pi$, red). Also the eigenenergies of the full Hamiltonian and the experimental spectrum of ^{128}Cd are shown.

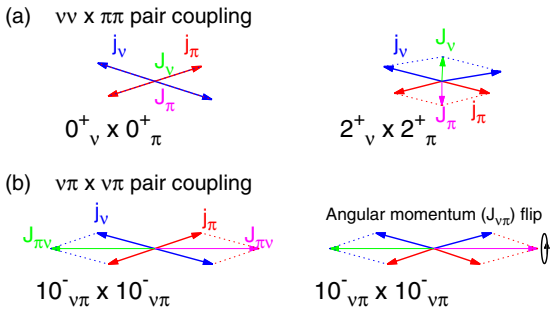

FIG. 4. Graphical illustration of the (a) $\nu\nu$-$\pi\pi$ and (b) $\nu\pi$-$\nu\pi$ basis for a 0^+ state. The dashed lines indicate the angular momentum vector adding scheme for different pairs. In (b) both couplings are identical but one pair is spin-flipped around its total angular momentum axis.

and with the full Hamiltonian is remarkable for jj45pna and SDI. The FAP dominance is still observed for the quadrupole interaction albeit to a lesser extent. With reference to Fig. 1 it is clear that the driving force behind the mechanism of the FAP dominance is the TBME for $J_{\nu\pi} = j_\nu + j_\pi$ since for the schematic quadrupole interaction this matrix element is less attractive than it is for jj45pna or SDI.

The dominant components of the 0^+_1 and 2^+_1 states resulting from the complete jj45pna calculation are

$$|0^+_1\rangle \approx 0.82|0_\nu 0_\pi; 0\rangle + 0.52|2_\nu 2_\pi; 0\rangle + \cdots ,$$
$$|2^+_1\rangle \approx 0.62|2_\nu 0_\pi; 2\rangle + 0.56|0_\nu 2_\pi; 2\rangle - 0.36|2_\nu 2_\pi; 2\rangle + \cdots ,$$

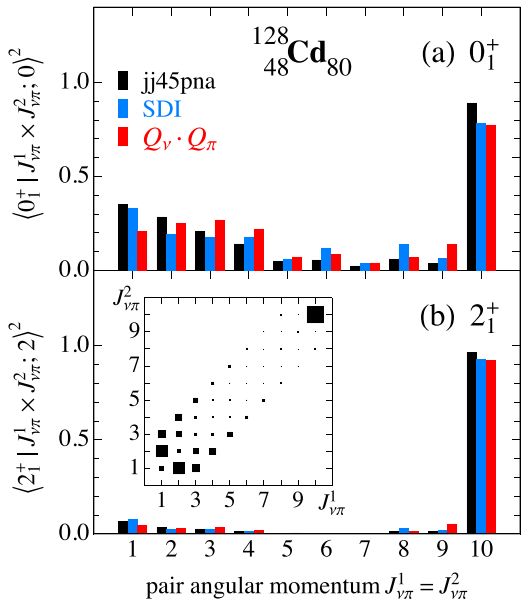

FIG. 5. Squares of the components of the yrast eigenstates of ^{128}Cd expressed in the $\nu\pi$-$\nu\pi$ basis $|J^1_{\nu\pi} J^2_{\nu\pi}; J\rangle$ for (a) $J = 0$ and (b) $J = 2$. The main figure shows $\langle J_1 | J^1_{\nu\pi} J^2_{\nu\pi}; J\rangle^2$ as a function of $J^1_{\nu\pi} = J^2_{\nu\pi}$ for three different $\nu\pi$ interactions: (i) realistic (jj45pna, black), (ii) surface delta (SDI, blue), and (iii) quadrupole ($Q_\nu \cdot Q_\pi$, red). In the inset of (b) this quantity is shown (for jj45pna) as proportional to the size of the squares as a function of $J^1_{\nu\pi}$ and $J^2_{\nu\pi}$.

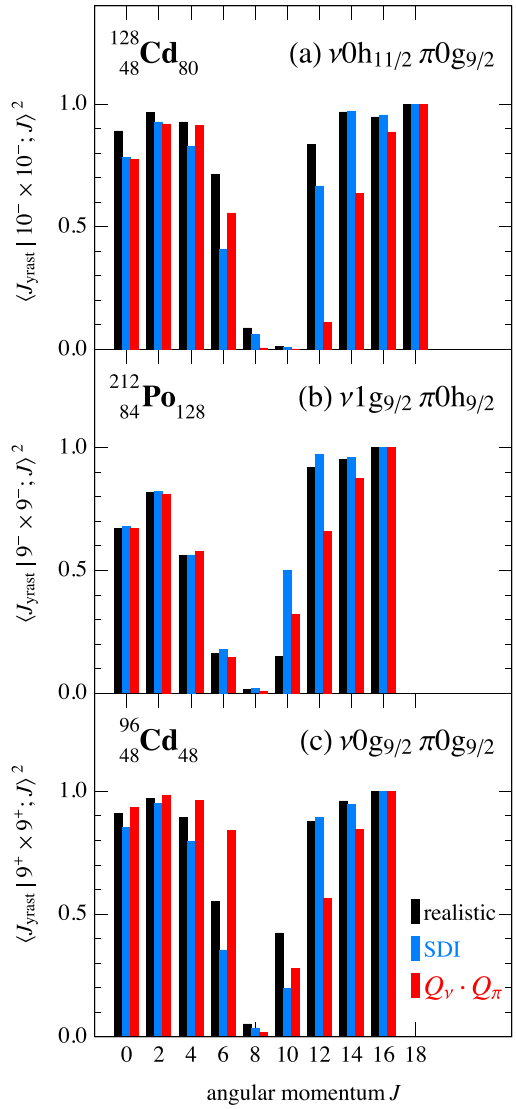

FIG. 6. Overlaps $\langle J_{\rm yrast} | (J^{\rm FAP}_{\nu\pi})^2; J\rangle^2$ as a function of the angular momentum J for (a) ^{128}Cd, (b) ^{212}Po, and (c) ^{96}Cd calculated with a realistic interaction (black), and compared to the surface delta (SDI, blue) and quadrupole ($Q_\nu \cdot Q_\pi$, red) interactions.

while those obtained with $V^{10^-}_{\nu\pi}$ only read

$$|0^+_1\rangle \approx 0.89|0_\nu 0_\pi; 0\rangle + 0.43|2_\nu 2_\pi; 0\rangle + \cdots ,$$
$$|2^+_1\rangle \approx 0.66|2_\nu 0_\pi; 2\rangle + 0.60|0_\nu 2_\pi; 2\rangle - 0.34|2_\nu 2_\pi; 2\rangle + \cdots .$$

Note the important $|2_\nu 2_\pi; 0\rangle$ component in the 0^+ ground state as well as the qualitative agreement of the wave functions in both calculations.

So far we have considered a pair of neutrons coupled to a pair of protons and found considerable mixing in the $\nu\nu$-$\pi\pi$ basis due to the $\nu\pi$ interaction. Alternatively, $\nu\pi$ pairs can be considered for the construction of a $\nu\pi$-$\nu\pi$ basis with vectors $|J^1_{\nu\pi} J^2_{\nu\pi}; J\rangle$ (see Supplemental Material [22]). It is important to realize that the $\nu\nu$-$\pi\pi$ basis is orthogonal whereas the $\nu\pi$-$\nu\pi$ basis is not. Also, the states in both bases may have large overlaps, depending on the coupling of the angular momenta. This is illustrated for the 0^+ state in Fig. 4, where states in

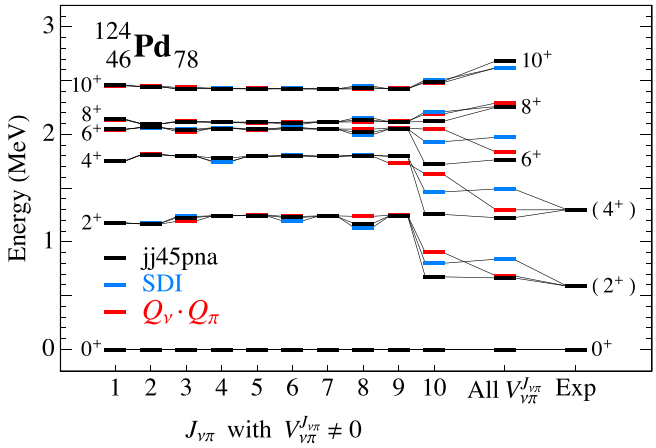

FIG. 7. Same as Fig. 3 but for four neutrons and four protons (^{124}Pd).

both bases are represented graphically, leading to similar or dissimilar configurations, as the case may be.

Figure 5 displays, for the three different $\nu\pi$ interactions, the squares of the components of the yrast eigenstates of the full Hamiltonian for ^{128}Cd, expressed in the $\nu\pi$-$\nu\pi$ basis $|J^1_{\nu\pi} J^2_{\nu\pi}; J\rangle$ for $J = 0$ and $J = 2$. We emphasize that the $\nu\pi$-$\nu\pi$ basis is nonorthogonal and therefore the sum of the squares may exceed 1. Nevertheless, from Fig. 5 it follows that, independent of the $\nu\pi$ interaction, the biggest and dominant contribution to the 0^+_1 and 2^+_1 states comes from the FAP with $J^1_{\nu\pi} = J^2_{\nu\pi} = J^{\rm FAP}_{\nu\pi}$. The low-$J_{\nu\pi}$ pairs have a non-negligible contribution to 0^+_1 but contribute little to 2^+_1. Further, the inset of Fig. 5(b) shows that the second strongest contribution to 2^+_1 results from $(J^1_{\nu\pi}, J^2_{\nu\pi}) = (1,2)$ [or (2,1)].

This analysis can be repeated for other yrast eigenstates of ^{128}Cd, as is done in Fig. 6(a), which shows, as a function of the angular momentum J of the state, the overlaps $|\langle J_{\rm yrast}|(J^{\rm FAP}_{\nu\pi})^2; J\rangle|^2$, where $|J_{\rm yrast}\rangle$ is an eigenstate of the full Hamiltonian. Again independent of the $\nu\pi$ interaction, the FAP is seen to give rise to the major component of the low- and high-J yrast eigenstates while its contribution is small at mid J. The $J = 8$ and $J = 10$ yrast eigenstates are fragmented in the $\nu\pi$-$\nu\pi$ basis and their structure is more transparent in the $\nu\nu$-$\pi\pi$ basis, where they correspond dominantly to a seniority $\upsilon = 2$ state, i.e., to $|0^+_\nu 8^+_\pi; 8^+\rangle$ and $|10^+_\nu 0^+_\pi; 10^+\rangle$, respectively.

To demonstrate the generic character of the results for ^{128}Cd, a similar analysis can be performed for different regions of the nuclear chart. In each case we consider a "realistic" interaction, taken from or fitted to data, and compare it with the surface delta and quadrupole interactions. The first example concerns ^{212}Po, which has two neutrons and two protons outside the closed-shell nucleus ^{208}Pb. Assuming that the neutrons are in $\nu 1g_{9/2}$ and the protons in $\pi 0h_{9/2}$, an effective interaction for this model space can be extracted from the observed spectra of $A = 210$ nuclei [26]. Figure 6(b) shows the overlaps $\langle J_{\rm yrast}|(J^{\rm FAP}_{\nu\pi})^2; J\rangle^2$ involving the FAP state with $J^{\rm FAP}_{\nu\pi} = 9$. The behavior is similar to that found in ^{128}Cd but at low J the FAP dominance is less pronounced. This illustrates the crucial role of the TBME in the FAP state, which is less attractive in ^{212}Po, owing to the combination of a neutron orbital with $j_\nu = \ell_\nu + 1/2$ and a proton orbital with $j_\pi = \ell_\pi - 1/2$ as compared to ^{128}Cd with $j_\nu = \ell_\nu + 1/2$ and $j_\pi = \ell_\pi + 1/2$. In addition, we present in Fig. 6(c) an application to an $N = Z$ nucleus, ^{96}Cd, where neutrons and protons occupy the same orbital $0g_{9/2}$, using the interaction from Ref. [27]. This case again is markedly similar to what is found in ^{128}Cd.

Finally, the above analysis can be extended to four neutrons and four protons. In Fig. 7 are shown the results for ^{124}Pd, obtained in the same way as those for ^{128}Cd in Fig. 3. Again we find that the results of the calculation with the FAP interaction are close to those obtained with the complete $\nu\pi$ interaction, which in turn are in close agreement with experiment [28]. This result for ^{124}Pd can be seen as the analog to that for ^{92}Pd [5]. The regularly spaced level sequence, claimed to be the experimental signature of the dominance of the FAP in ^{92}Pd [5], is also observed for ^{124}Pd.

We conclude therefore that, if valence nucleons dominantly occupy high-j orbitals, the yrast spectroscopy of the nucleus is essentially determined by a single matrix element, namely, the one where neutron and proton are fully aligned in angular momentum. This property can be considered as a generic feature of the neutron-proton interaction, akin to pairing between identical nucleons. Since the seminal papers of Racah and Elliott, one of the friendly companions of nuclear spectroscopists has been the pairing-plus-quadrupole model. With this study we suggest that the mechanism at the basis of the success of this schematic Hamiltonian is the interaction in the configuration with fully aligned neutron and proton angular momenta and that therefore a study of possible symmetries of the pairing-plus-FAP model is called for.

[1] E. H. Lieb and F. Y. Wu, Phys. Rev. Lett. **20**, 1445 (1968).
[2] J. Dukelsky, S. Pittel, and G. Sierra, Rev. Mod. Phys. **76**, 643 (2004).
[3] G. Racah, Phys. Rev. **63**, 367 (1943).
[4] J. P. Elliott, Proc. Roy. Soc. (London) A **245**, 128 (1958).
[5] B. Cederwall *et al.*, Nature **469**, 68 (2011).
[6] C. Qi *et al.*, Phys. Rev. C **84**, 021301 (2011).
[7] Z. Xu *et al.*, Nucl. Phys. A **877**, 51 (2012).
[8] M. Danos and V. Gillet, Phys. Rev. **161**, 1034 (1967).
[9] S. Zerguine and P. Van Isacker, Phys. Rev. C **83**, 064314 (2011).
[10] P. Van Isacker, Int. J. of Mod. Phys. E **22**, 1330028 (2013).
[11] K. Neergård, Phys. Rev. C **88**, 034329 (2013).
[12] K. Neergård, Phys. Rev. C **90**, 014318 (2014).
[13] L. Zamick and A. Escuderos, Phys. Rev. C **87**, 044302 (2013).
[14] G. J. Fu, Y. M. Zhao, and A. Arima, Phys. Rev. C **88**, 054303 (2013).
[15] G. J. Fu, Y. M. Zhao, and A. Arima, Phys. Rev. C **90**, 054333 (2014).
[16] L. Coraggio, A. Covello, A. Gargano, and N. Itaco *et al.*, Phys. Rev. C **85**, 034335 (2012).
[17] G. J. Fu, J. J. Shen, Y. M. Zhao, and A. Arima, Phys. Rev. C **87**, 044312 (2013).
[18] G. J. Fu, Y. M. Zhao, and A. Arima, Phys. Rev. C **91**, 054322 (2015).

[19] M. Sambataro and N. Sandulescu, Phys. Rev. C **91**, 064318 (2015).
[20] S. Robinson, M. Harper, and L. Zamick, arXiv:1411.1390v5.
[21] S. Frauendorf and A. Macchiavelli, Prog. Part. Nucl. Phys. **78**, 24 (2014).
[22] See Supplemental Material at http://link.aps.org/supplemental/10.1103/PhysRevC.97.041302 for explicit description of TBME and transformation from $\nu\nu$-$\pi\pi$ basis to $\nu\pi$-$\nu\pi$ basis.
[23] M. Rejmund *et al.*, Phys. Lett. B **753**, 86 (2016).
[24] M. Hjorth-Jensen, T. T. Kuo, and E. Osnes, Phys. Rep. **261**, 125 (1995).
[25] A. P. Zuker, A. Poves, F. Nowacki, and S. M. Lenzi, Phys. Rev. C **92**, 024320 (2015).
[26] M. S. Basunia, Nucl. Data Sheets **121**, 561 (2014).
[27] F. Serduke, R. Lawson, and D. Gloeckner, Nucl. Phys. A **256**, 45 (1976).
[28] H. Wang *et al.*, Phys. Rev. C **88**, 054318 (2013).